Journal of Materials Chemistry A

Accepted Manuscript

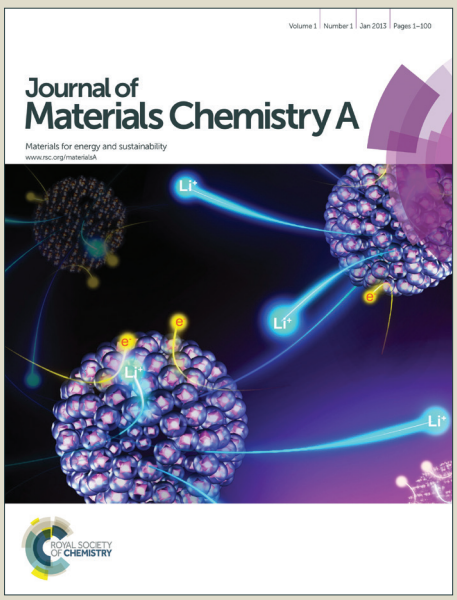

ROYAL SOCIETY OF CHEMISTRY

www.rsc.org/materialsA

EXAFS and FTIR studies of selenite and selenate sorption by alkoxide-free sol-gel generated Mg-Al-CO_3 layered double hydroxide with very labile interlayer anions

Natalia Chubar[12*]

Abstract

Current research on Layered Double Hydroxides (LDHs, also known as Hydrotalcites, HTs) is predominantly focused on their intercalations, but the industrial application of LDHs for anion exchange adsorption has not yet been achieved. It was recently recognized that, to develop LDH applications, these materials should be produced using methods other than direct co-precipitation. Mg-Al-CO_3 LDH produced using an alkoxide-free sol-gel synthesis showed exceptional removal properties for aqueous selenium species. Se K-edge EXAFS/XANES and FTIR studies (supporting the data by XRD patterns) were performed to explain the unusual adsorptive performance of Mg-Al LDH by revealing the molecular-level mechanism of $HSeO_3^-$, SeO_4^{2-} and $\{HSeO_3^-+SeO_4^{2-}\}$ uptake at pH 5, 7 and 8.5. The role of inner-sphere complexation (exhibited by inorganic adsorbents with good performance) in adsorption of both selenium aqueous species was not confirmed. However, Mg-Al LDH fully met the other expectations regarding the involvement of the interlayer anions. The interlayer carbonate (due to its favorable speciation and generous HT hydration) gave a "second breath" to selenite sorption and was the only mechanism that controlled the removal of Se(VI). Because inner sphere complexation was the leading mechanism for selenite removal, ion exchange via surface OH^- and interlayer CO_3^{2-} species was the only mechanism for selenate removal; both of these species were easily bound to Mg-Al LDH (on its surface and gently parked into the interlayer forming a multilayer without violation of the structure of Mg-Al-CO_3 LDH). This work provides the first theoretical explanation of why it is more difficult to sorb selenate than selenite and which material should be used for this purpose.

Introduction

Layered double hydroxides (LDHs), also known as anionic nanoclays or hydrotalcites (HTs), are two-dimensional, elegantly structured inorganic materials. Their general formula is

$$[M^{2+}_{1-x}M^{3+}_{x} \times (OH)_2]^{x+}(A^{n-})_{\frac{x}{n}}.\, mH_2O$$

where M^{2+} usually represents metallic divalent cations, such as Mg, Fe(II), Co(II), Zn and Mn(II), and M^{3+} typically represents trivalent cations, such as Al and Fe(III) [1]. Many other chemical compositions of LDHs with various layers and/or interlayers have been developed.[1-6]

Because the possibility for multiple uses (in variety of technologies) is one of the criterions for a material to be sustainable, LDHs are a typical example of a sustainable material. They attract great interest due to their potential as ion exchangers and adsorbents; catalysts and catalyst supports; delivery carriers and hosts for a variety of medicines, cosmetics and pharmaceuticals; CO_2 scavengers and additives to plastics, building materials and others.[1-6] One of the latest focuses is health-related applications, including the development of pharmaceutical formulations for cancer therapy.[7]

One of the most obvious and easiest applications of LDHs (using only generic materials without calcination, intercalation, impregnation, reconstruction or other pre-treatments) is the removal of anions from water. A superior anion removal capability is expected due to the double anion exchange capacity of a material with this type of structure. The interlayer ions are expected to be involved in the removal of toxic anions additionally to surface OH^- groups. However, since 1842, when HTs were first discovered, they have not been applied as anion exchangers in industrial scales. Instead, researchers usually focus on the intercalation and preparation of various hybrid HT materials.[1,6,8,9]

HTs have not yet been implemented at industrial facilities due to their low performance; they have not met the expectations of water engineers and separation technology professionals.[10-11] Translating the disappointment of engineers into (molecular-level) chemistry language, the low removal capabilities of LDHs toward target (for water industries) anions is mainly due to the

unsatisfactory behavior of the interlayer anions. Instead of active participation in the removal process, most of them are completely inert because they are strongly bound to the sheets by bidentate coordination.[11] The ability of interlayer ions to be easily exchangeable must be provided by the synthetic method. The most popular synthetic method, namely direct precipitation of two salts (used by >90% of the researchers and by most industries producing these materials), does not provide this property to HTs.[11-12]

General awareness that HT preparation methods should be improved is growing[12-13] and has resulted in a few recent elaborations of HT syntheses.[13-14] One of the new methods (based on using organic solvents) produces tripodal-ligand-stabilized layered double hydroxide nanoparticles with highly exchangeable CO_3^{2-}.[13] Another work is an elaboration by the authors. Their synthetic approach (based on pure inorganic synthesis) also produces Mg-Al-CO_3 LDHs with highly exchangeable CO_3^{2-}.[11,14] It is a cost-effective, environmentally friendly and easy to upscale preparation method (with the inclusion of an alkoxide-free sol-gel synthesis) and produces Mg-Al LDH with the highest anion removal capacity for toxic anions.[11,14]

Selenium is a well-known chemical element due to its dual properties. It is an important nutrient for living organism and therefore a constituent of many food supplements. Thus, recovery of selenium (an expensive substance) from wastewaters is an important technological task. In contrast, high concentrations of selenium are toxic, which result in a lowering of its maximum permissible concentration by the WHO to very difficult to achieve levels of 10 μg/L. Due to the low performance of many adsorbents toward selenium species (especially selenate, which is the main species in surface waters), technical reports conclude that adsorption is not a suitable technological approach for the removal and recovery of selenite and, especially, selenate.[15]

The selenium removal performance of the Mg-Al LDH developed by the authors contradicts the conclusions from the pilot-scale testing.[15] To explain the high adsorptive capabilities of Mg-Al LDH, the authors conducted studies on the mechanism of selenate and selenite sorption by EXAFS and FTIR as a function of pH. The results are shown in this work, which is also the first EXAFS

study of selenite and selenate sorption using layered double hydroxides. It is also the first work to investigate the simultaneous sorption of Se(VI) and Se(IV) by an adsorbent.

High adsorptive performance by inorganic ion exchangers is usually explained using a chemisorption mechanism. If an inorganic ion exchanger has a layered structure, the expectation for such material is to host excess toxic anions in its interlayer space (not demonstrated by most HTs). The goals of this work were to use FTIR and EXAFS (supporting the data by XRD patterns) to (1) define the role of the interlayer carbonate in the removal process of selenite, selenate and their mixture at various pH values (5, 7 and 8.5) and (2) reveal if chemisorption is really a mechanism for both selenite and selenate sorption at pH = 5, 7 and 8.5.

Experimental Section

Synthesis. Mg-Al LDH with carbonate interlayer ions was prepared via an alkoxide-free sol-gel synthesis method. This synthesis is described in detail in the previous paper[14]. The synthesis was based on the following principles: include a sol-gel route in the synthesis strategy, avoid the direct precipitation of Mg and Al hydroxides and preserve high hydration and an abundance of surface OH^-. These tasks were achieved in a step-wise manner. The sol-gel routes were preserved during the hydrolysis of $AlCl_3$. A hydrogel of aluminum hydroxide already contained the second metal cation, which was hydrolyzed later. The layered structure was tailored during the final stage of the synthesis together with the hydrolysis of the second salt, $MgCl_2$. The thermal treatment, which is usually expected in the preparation strategy of any adsorbent (to make it strong enough for water treatment), was included in the xerogel treatment, but the temperature was not very high (155-160 °C), which allowed the surface to retain many OH^- groups. The main stages of the material preparation are shown below:

1). $Mg(HCO_3)_2$ was synthesised using a solution of $MgCl_2 \cdot 6H_2O$ and solid $NaHCO_3$:

$$MgCl_2 \cdot 6H_2O + 2NaHCO_3 = Mg(HCO_3)_2 + 2NaCl + 6H_2O \quad (1)$$

2) Suspension of the freshly synthesised $Mg(HCO_3)_2$ was placed into contact step-wise with an $AlCl_3$ solution, which was constantly stirred with a magnetic stirrer at 290-330 rpm, which led to the formation of a hydrogel at the end of the reaction.

$$2AlCl_3 \cdot 6H_2O(solution) + 3Mg(HCO_3)_2(suspension\_containini ng\_NaCl) \xrightarrow{sol-gelation-gel} 2Al(OH)_3 \cdot nH_2O\_[hydrogel\_containing\_Mg^{2+}, Na^+, Cl^-, HCO_3^-] \quad (2)$$

The hydrogel was aged for 24 hours in glass beaker, moved out of the beaker and left at ambient temperature for drying till it become xerogel. Xerogel was treated thermally at 155-160 ^oC for 48 hours increasing the temperature slowly step-wise from 60 to 160 ^oC. It was then cooled down till the room temperature and was slowly added to (stirred) water solution of strong base(s) at pH=10.3. pH was adjusted during the reaction until stable. Any strong base (Na_2CO_3, K_2CO_3, NaOH, KOH, NH_4OH or mixture of them) can be used. It always leads to formation of Mg-Al-CO_3 LDH as carbonate was already inside of xerogel. The final product (Mg-Al-CO_3 LDH) was filtered and washed.

Adsorption studies. Equilibrium isotherms of selenite and selenate adsorption were obtained in batches at a standard adsorbent dose of 2 g/L (using stock solutions of Na_2SeO_3 and Na_2SeO_4 and varying the initial concentration from 5 to 500 mg [Se]/L) at 22±2 °C. The pH was adjusted using 0.1 N NaOH and HCl. The background electrolyte was 0.01 NaCl. The adsorptive capacity was calculated using

$$q = \frac{(C_o - C_{eq.})V}{m}, \quad (1)$$

where q (mg/g_{dw}) is the amount of selenium sorbed per gram of dry weight of the adsorbent, C_o (mg/L) is the initial concentration of Se, C_{eq} (mg/L) is the final (or equilibrium) concentration of the anion in solution, V (L) the volume of solution and m (g_{dw}) is the dry mass of the adsorbent.

Preparation of the samples for FTIR and EXAFS. Mg-Al LDHs with sorbed Se were prepared for spectroscopy studies separately to have enough of the materials for EXAFS in the transmission mode and to study the Se bound to Mg-Al LDH saturated with these anions. Three sets of the experiments were conducted. First, 500 mg [Se]/L of selenite, selenate and a mixture of these

two anions (250 mg [Se]/L of each) in 0.01 N NaCl were exposed to the solids (at the adsorbent dose of 2 g/L) and kept on a shaker until equilibrium was reached. The pH was adjusted regularly. The solids were filtered using 0.4-μm membrane filters and dried in air at ambient temperature.

Chemical analysis: The concentrations of Se were analyzed using inductively coupled plasma atomic emission spectroscopy (ICP-AES).

Fourier Transform Infra-Red (FTIR) spectra were collected using a Nicolet 6700 FTIR spectrometer (Nicolet Co., USA) in the transmission mode for wavenumbers from 400 to 4000 cm^{-1}. The samples were dried and prepared in spectral-grade KBr. All IR spectroscopy measurements were performed at ambient temperature.

XANES/EXAFS. The Se K-edge spectra (12658 eV) were recorded in the transmission mode at the ambient temperature at DUBBLE (BM26A) at ESRF.[16] The monochromator was calibrated assigning an energy value of 12658 eV to the first inflection point in the absorption edge. The nine experimental samples of HTs with sorbed selenite, selenite and both selenium aqueous species (collected at pH 5, 7 and 8.5) and the experimental references (Na_2SeO_3 and Na_2SeO_4) were grinded to very fine powders, mixed with boron nitride and prepared as pellets. The optimal percentage of selenium in each sample was calculated. IFFEFIT (Athena, Artemis and Atoms) programs were used for the data analysis, treatment and modeling.[17] FEFF9 was used to generate feff.inp files for analysis by Artemis using the atomic coordinates of the relevant theoretical references calculated by X-ray crystallographic methods available in the literature: $Al_2(SeO_3)_3 \cdot 3H_2O$[18], $MgSeO_3 \cdot 2H_2O$[19], $[Al(H_2O)_6]_2(SeO_4)_3(H_2O)_4$[20], $[Al_2(OH)_2(H_2O)_8](SeO_4)_2 \cdot 2H_2O$[21], anhydrous $Al_2(SeO_4)_3$[22] and $MgSeO_4 \cdot 6H_2O$[23] .

X-ray Diffraction (XRD) Patterns were collected by a Bruker-AXS D8 Advance powder X-ray diffractometer, equipped with an automatic divergence slit, Vantec-1 detector, and cobalt $K\alpha 1,2$ (λ = 1.79026 A) source.

Results

The material. The surface chemistry and structure of the Mg-Al LDHs were characterized in detail in the previous work.[11,14] In summary, the original Mg-Al LDHs (without any calcination or other treatments) have high (for inorganic adsorbents) specific surface areas (180-250 m^2/g) and a mesoporous structure.[11,14] The Mg/Al ratio on the surface of the material is different from that in the bulk. Mg is abundant on the surface, which increases the basicity of Mg-Al LDH. The number of different species (aluminum, magnesium and interlayer carbonate) of the Mg-Al LDH is greater than the other LDHs prepared using different syntheses[11], which increases the material heterogeneity and reactivity in general (and lead to easier carbonate exchangeability). In addition, it is a highly hydrated material (30-35% water). In summary, Mg-Al LDH has very important properties for an inorganic ion exchanger to remove toxic anions (very competitively).

Adsorption of selenium oxyanions. Fig. 1 (isotherms of selenite (A) and selenate (B) adsorption at pH 5, 7 and 8.5, and comparison of selenite (C) and selenate (D) removal performances of various materials) shows that Mg-Al LDH has excellent adsorptive properties toward selenate and selenite. It shows not only the highest capacity (plateau of the curve) but also the highest affinity (steep-type isotherms) toward both selenite and selenate, which makes the material promising for both applications: the recovery of selenium from wastewater (when a high capacity is necessary) and water treatment (when this chemical element shall be reduced to 10 µg/L, which can be performed by an adsorbent with a very high affinity toward selenium species). The selenate removal capacity is an especially attractive capability of Mg-Al LDH because it is much more difficult to remove selenate than selenite, but selenate is the main aqueous species in surface waters.

The adsorption of selenate and selenite was subjected to a general trend in the pH dependency for anion exchange adsorption (a lower pH is associated with a higher adsorption). An increase of H^+ in solution facilitates the anion exchange of surface OH^-, which usually results in a higher adsorption (at lower pH values).

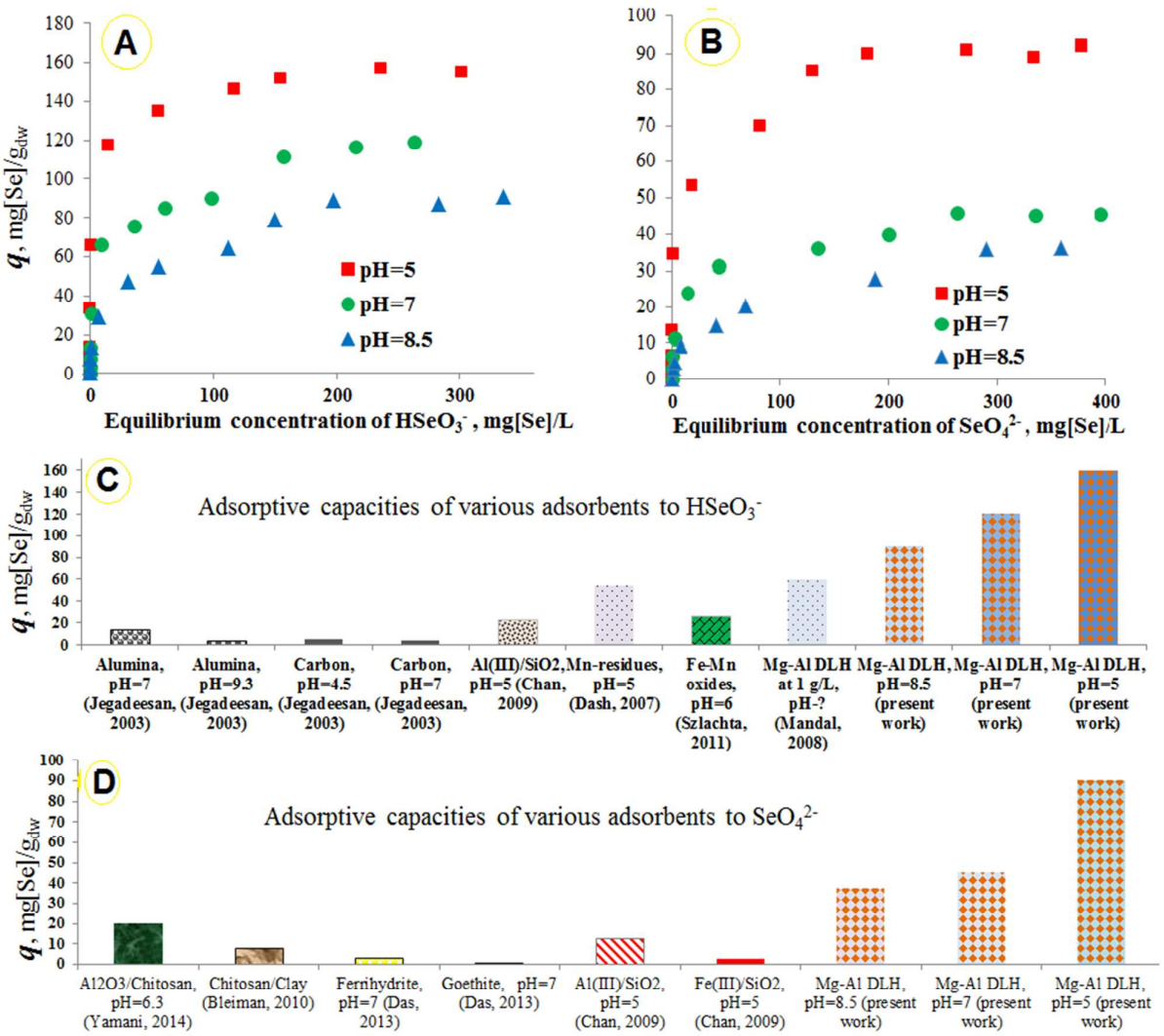

Fig. 1. Isotherms of selenite (A) and selenate (B) adsorption by Mg-Al-CO_3 LDH at the adsorbent dose of 2 g/L, 22±2 °C and constant pH of 5, 7 and 8.5 and comparison of the adsorptive capacities of various materials toward selenite (C) and selenate (D) based on the literature.[25-33]

However, the adsorptive removal performance of Mg-Al LDH at pH 5, 7 and 8.5 does not correlate strictly with the *E*h-pH diagram data.[24] Selenite at pH 5 is $HSeO_3^-$ (the species with the highest adsorptive ability); at pH= 7, two species, $HSeO_3^-$ and SeO_3^{2-}, co-exist; and at pH=8.5, selenite is mainly SeO_3^{2-} (the species with the lowest adsorptive ability). The selenite removal capacity of Mg-Al LDH was 80, 120 and 160 mg [Se]/g_{dw} at pH 8.5, 7 and 5 (Fig. 1A).

The selenate species at pH > 2 are SeO_4^{2-}.[24] Selenate was sorbed by this material at capacities of 30, 45 and 90 mg [Se]/g_{dw} at pH 8.5, 7 and 5, respectively (Fig. 1B). This high removal capacity toward selenate cannot be explained by its speciation as a function of pH because selenate exists in water as SeO_4^{2-}, which is the most difficult species for adsorptive removal. As for the pH effect, the increase in H^+ (at the lower pH values) cannot in principle increase the adsorption from 45 up to 90 mg [Se]/g_{dw}, which indicates another major mechanism of its adsorption by Mg-Al LDH. Obviously, the same mechanism was not possible for commercial inorganic ion exchange adsorbents, such as granulated ferric hydroxide (GFH) and activated alumina (AA), and most likely many other materials.

There is little research in the literature on the adsorptive removal of selenite and selenate at pH≥7 due to the very low adsorptive capacities of the investigated materials. Figs. 1C and D show how the different adsorptive properties of Mg-Al LDH materials toward both selenite and selenate compare with those of various other adsorbents.

FTIR spectroscopy studies. Fig. 2 shows the results of the FTIR examination of the initial Mg-Al LDH and with sorbed selenite (2A), {selenite+selenate} (2B) and selenate (2C) at pH 5, 7 and 8.5. The initial adsorbent shows all of the main features of layered double hydroxides. Many bands from 413 to 942 cm^{-1} originate from metal-oxygen-metal vibrations. The strong signals at 413 cm^{-1} (δ O-M-O) are characteristic of the lattice vibrations of [Mg, Al] octahedral sheets (as $[AlO_6]^{3-}$), which provides evidence for the formation of the typical phases of layered double hydroxides. [33] The Mg/Al-OH and Al-OH translations are found at 760-780 cm^{-1}.[33,34] The strong bands at 3442 cm^{-1} are stretching bands of the hydrogen-bonded hydroxyl groups and H_2O from both the surface and interlayer (Fig. S1, Supplementary Information (SI)). The broadness of this band indicates few types of OH^- coordination. The sufficient hydration of the interlayer is reflected at 1635 cm^{-1} and assigned to the interlayer water deformation bands (δ(H_2O)).

.

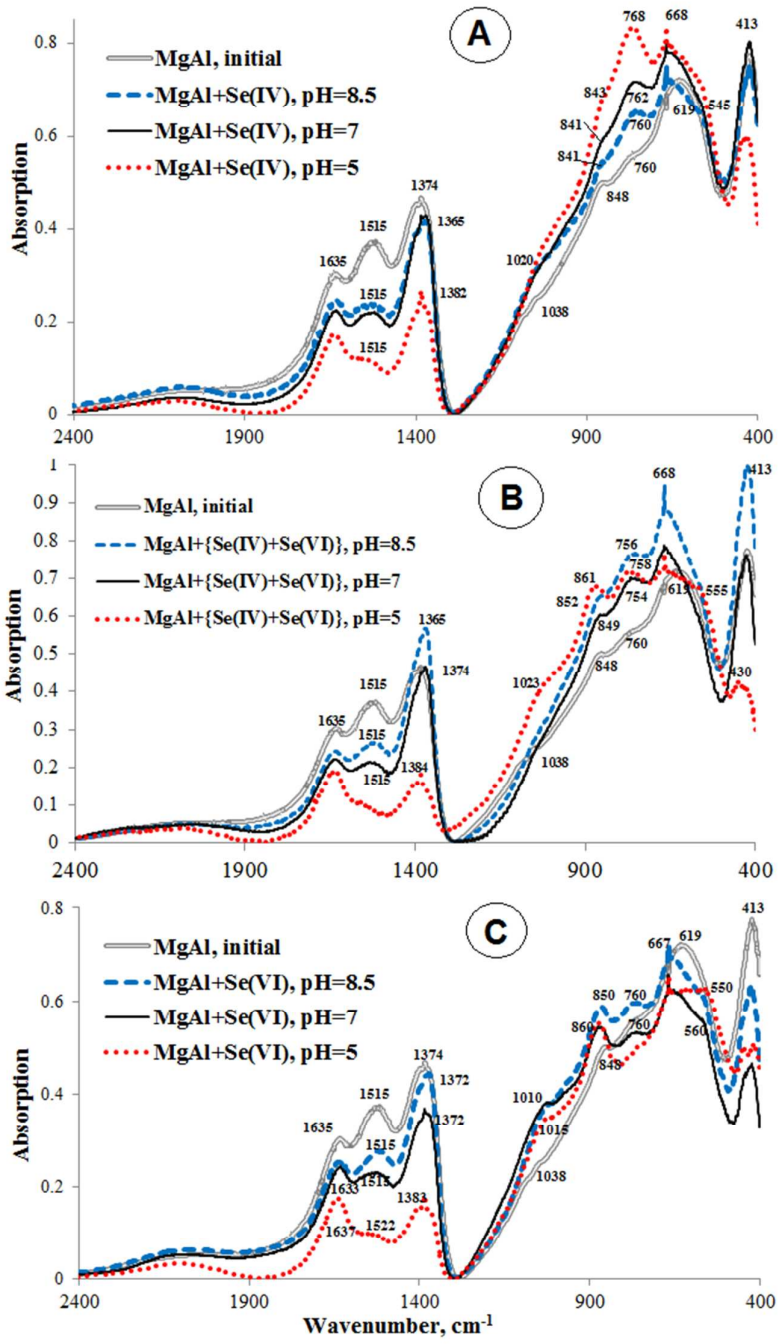

Fig. 2. FTIR spectra of Mg-Al LDH with sorbed selenite (A), two selenium aqueous species (selenite+selenate) (B) and selenate (C) at pH 5, 7 and 8.5. Experimental conditions: the initial selenium concentration was 500 mg [Se]/L and the adsorbent dose was 2 g/L at 22±2 °C.

The presence of ionic carbonate in the interlayer space of the initial adsorbent is reflected in the IR active absorption bands at 1374 (γ3), 1515 and 848 cm^{-1}, which indicate the presence of

carbonate species. The band at 1515 cm^{-1} was assigned to the asymmetric bending vibrations of CO_3^{2-} and was interpreted as monodentate-coordinated ions.[10,33] The peak at 848 cm^{-1} was assigned to the symmetric stretching of carbonate with bidentate coordination.[35,36] The strongest band at 1374 cm^{-1} can be assigned to both bidentate or monodentate carbonate[10], but based on the adsorption data (shown in this work), its mobility/exchangeability is lower than the lability of the carbonate species reflected at 1515 cm^{-1}.

$HSeO_3^-$ is represented in the FTIR spectra by the bands at 760, 762 and 768 cm^{-1}, which are larger at the lower pH values (Fig. 2A), reflecting the pH effect of selenite sorption (Fig. 1A). The shoulders at 841-843 cm^{-1} should also be assigned to selenite vibrations.[37]

In the FTIR spectra of Mg-Al LDH with sorbed selenate, the bands at 850-860 cm^{-1} should be attributed to ν(Se-O) vibrations of Se(VI)-O-Al/Mg complexes (Fig. 2C).[37,38] Interestingly, SeO_4^{2-} is shown at 850 and 860 cm^{-1} at pH 8.5 and 7/5 correspondingly.

The presence of both selenate and selenite are reflected by the bands: a stronger band at 754-758 cm^{-1} (assigned to Se(IV)) and a smaller one at 849-862 cm^{-1} (assigned to Se(VI)) (Fig. 2B). It is obvious that Mg-Al LDHs contain both selenate and selenite even at pH 8.5 when, due to their different adsorptive capacity, selenite might have completely dominated selenate.

The adsorption of selenate, selenite and both species together resulted in significant changes in the FTIR spectra in the region from 400 to 2000 cm^{-1}. Additionally, to decrease the bands assigned to OH^- (3442 and 1638 cm^{-1}) caused by the initial (and initiating) adsorption process via the anion exchange of OH^-, there was an obvious involvement of the interlayer carbonate in the removal of selenite, selenate and both ions together at pH 5, 7 and 8.5. However, the involvement of the interlayer ions was a function of the pH and the selenium aqueous species. The general (and expected) trend was the following: a lower pH was associated with a stronger involvement of the interlayer carbonate. In spite of the lower removal capacity of Mg-Al LDH toward SeO_4^{2-} than toward $HSeO_3^-$, the interlayer carbonate was more intensively involved in the removal of selenate, which is reflected in a more significant decrease in the bands at 1515 and 1774 cm^{-1} in the FTIR of

HTs with sorbed selenate (Figs. 2A and 2C). At pH 8.5, mainly monodentate carbonate (1515 cm^{-1}) was involved in the removal of both selenite (A) and selenate (C). At pH 7, both mono- and bidentate (1374 cm^{-1}) carbonate species participated in the removal of selenate, but only monodentate interlayer carbonate (1515 cm^{-1}) was involved in selenite removal. At pH 5, the bidentate carbonate species were involved in the removal of selenate more intensively than selenite, which is reflected in greater decrease of the band at 1374 cm^{-1} in the spectrum with selenate (Fig. 2C). The decrease in the carbonate bands resulted from the sorption of selenate, which was (visually) proportional to the adsorptive capacity of this ion as a function of pH (Figs. 1B and 2C). In contrast, the involvement of carbonate in the removal of selenite was nearly the same at pH 7 and 8.5 in spite of the quite different adsorptive capacities (Fig. 1A and 2A).

The influence of selenium adsorption on the layered structure of Mg-Al LDH is also reflected at 900-1100 cm^{-1}. The new bands in the spectra of HTs with sorbed anions at 1010-1020 cm^{-1} should be assigned to the interlayer carbonate vibrational modes[10], which became infrared active after the replacement of carbonate by selenate and selenite. These bands are stronger in the FTIR spectra of HTs with sorbed Se(VI) (Fig. 2C) and less distinguishable in the spectra of HTs with sorbed Se(IV) (Fig. 2A). In the spectra of the samples with both anions sorbed at pH 7 and 8.5, these bands are absent, but they are distinguishable at pH 5 (Fig. 2B). At pH 7 and 8.5, the interlayer hosted both anions, reaching saturation while still preserving the original layered structure of Mg-Al LDHs.

The sorption of selenium aqueous species caused considerable changes in the FTIR spectra in the region of the lattice vibrations of [Mg, Al] octahedral sheets (as $[AlO_6]^{3-}$) (413-900 cm^{-1}). Instead of a broad band at 619 cm^{-1} (the initial adsorbent), strong bands at 668 cm^{-1} appeared after the sorption of selenite, selenate and their mixture. Other new bands in the same region were noted at 550-555 cm^{-1}. These smaller bands were stronger at lower pH values. The bands at 667 and 556 cm^{-1} were assigned to vibrations of pure γ-Al_2O_3.[39] They can also be assigned to Mg-O vibrations in the region of 400-650 cm^{-1}.[34] Parker assigned the bands at 668 cm^{-1} in the FTIR of layered double

hydroxides to Mg-OH translation and the band at 550-555 cm^{-1} to Al-OH translations [10]. In addition, the band at 760 cm^{-1}, which was present in the FTIR of the initial Mg-Al LDH (reflecting Mg/Al-OH translations), became more distinguishable after the sorption of Se(VI) (Fig. 2C).

XANES. Fig. 3 shows the XANES of Mg-Al LDHs contacted to Se(IV) (A), Se{(IV)+(VI)} (B) and Se(VI) (C) at pH 5, 7 and 8.5 plotted together with the references, Na_2SeO_3 and Na_2SeO_4.

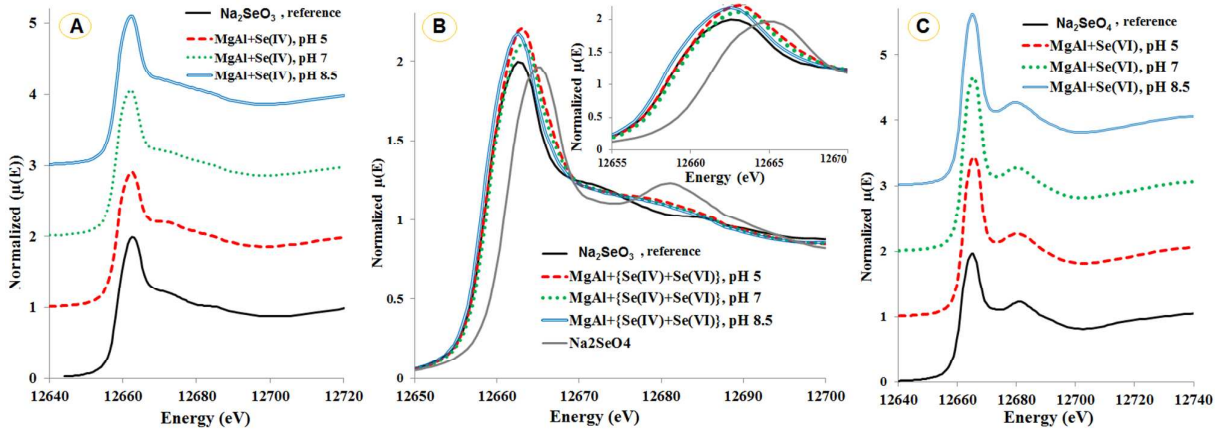

Fig. 3. XANES of Se-containing samples resulting from selenite (A), {selenite+selenate} (B) and selenate (C) sorption by Mg-Al LDHs at pH 5, 7 and 8.5. Experimental conditions: the initial selenium concentration was 500 mg [Se]/L and the adsorbent dose was 2 g/L at 22±2 °C.

The absorption edge positions measured using Se-XANES indicated that there was no change in the oxidation states during the adsorption of pure selenite (A) and selenate (C). Fig. 3B demonstrates that both aqueous selenium species, selenite and selenate, were sorbed to Mg-Al LDH at pH 5, 7 and 8.5. It is also obvious that the Se(IV)-to-Se(VI) ratio of the sorbed selenium species depends on the pH. The portion of Se(VI) was smallest at pH 8.5 and largest at pH 5, as reflected by the relevant (strong white line) peak positions which were at 12662 eV for Se(IV), 12665 eV for Se(VI), and in the case of both sorbed anions at 12662.6, 12663.1 and 12663.7 eV for pH 8.5, 7 and 5 respectively. The ratio of Se(IV)-to-Se(VI) in Mg-Al LDH exposed to both selenium species was

estimated using the Linear Combination fitting option of the Athena program. This estimation was rough because it was based on the references, Na_2SeO_3 and Na_2SeO_4, which do not take the second coordination shells into account, but it gave the results correlating with the Artemis fitting and FTIR studies. It was found that the portion of Se(VI) in the samples at pH 8.5, 7 and 5 was <10, 18 and 27%, respectively.

EXAFS studies. Fig. 4 shows the Se K-edge EXAFS of Se-containing Mg-Al LDHs resulting from batch adsorption equilibrium experiments at pH 5, 7 and 8.5. Fig. 4A and 4C show the EXAFS of HTs exposed to selenite or selenate, respectively. Fig. 4B shows the EXAFS of the Se-sorbed HTs exposed to both selenium species. Fig. 4 shows the k^2–weighted EXAFS, but both the k^2- and k^3-weighted EXAFS data were used for the fitting with Artemis (see Supporting Information) to ensure the correctness of the results. Fig. 4 confirms the conclusion of the XANES analysis that there was no change in the selenium oxidation state during adsorption. Fig. 4A and 4C show that selenium sorbed to Mg-Al LDH was correspondingly selenite (4A) and selenate (4C) as added to the experimental batches. Fig. 4B demonstrates that the selenite-to-selenate ratio in the solid state differs from the initial 50-50% ratio of selenite/selenate in the solution.

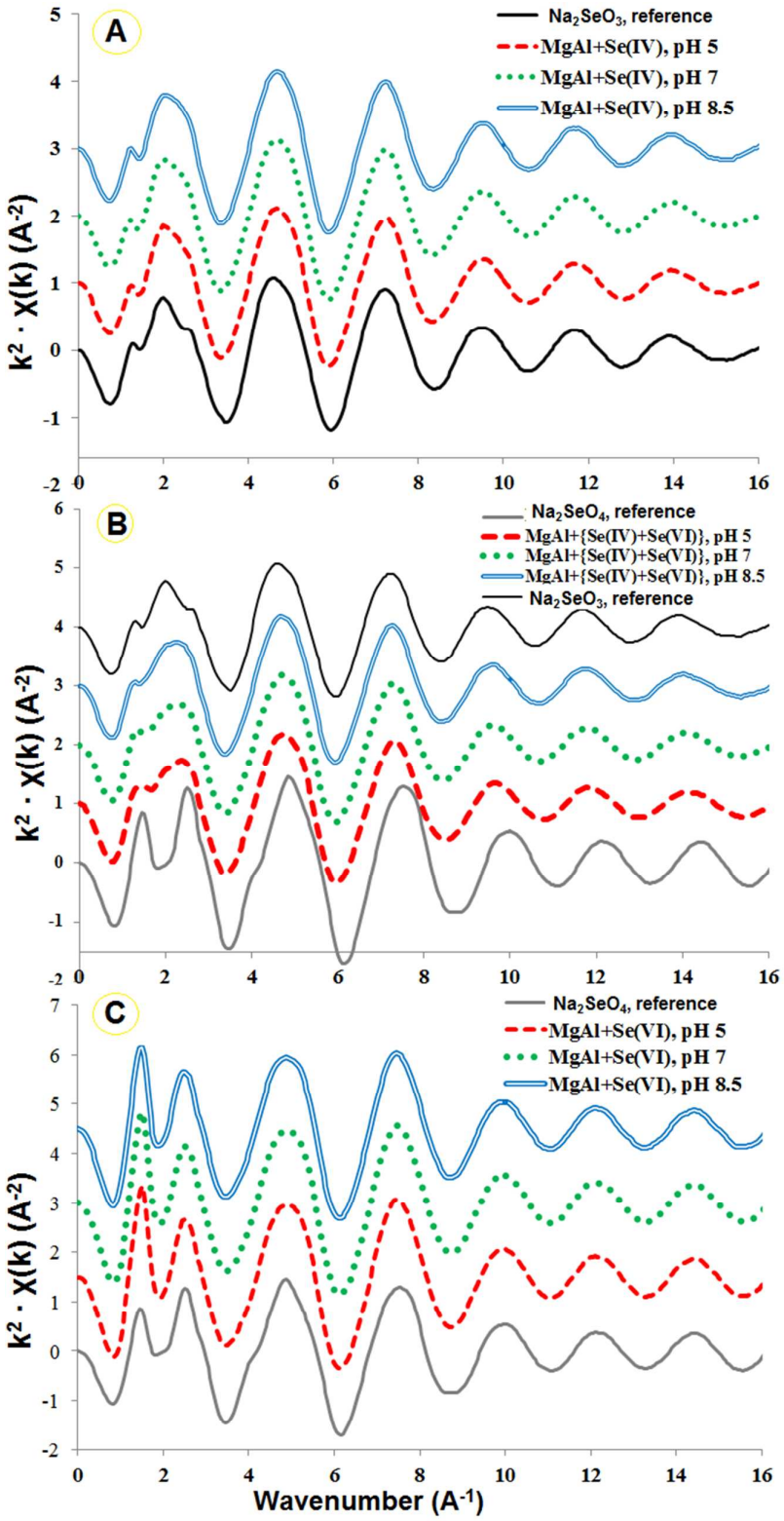

Fig. 4. Normalized Se K-edge EXAFS of Mg-Al LDHs with sorbed Se(IV) (A), Se{(IV)+(VI)} (B) and Se(VI) (C) at pH 5, 7 and 8.5. Experimental conditions: the initial selenium concentration was 500 mg [Se]/L and the adsorbent dose was 2 g/L at 22±2 °C.

Fig. 5 shows the radial structure functions around the Se atom (based on the corrected shifts) resulting from the Fourier transforms of the Se K-edge EXAFS of Mg-Al LDHs contacted to Se(IV)-(A(1)), {Se(VI)+Se(VI)}-(B(1)) and Se(VI)-(C(1)) at 0.3-6.0 Å and the second coordination shells of the same samples, A(2), B(2) and C(2).

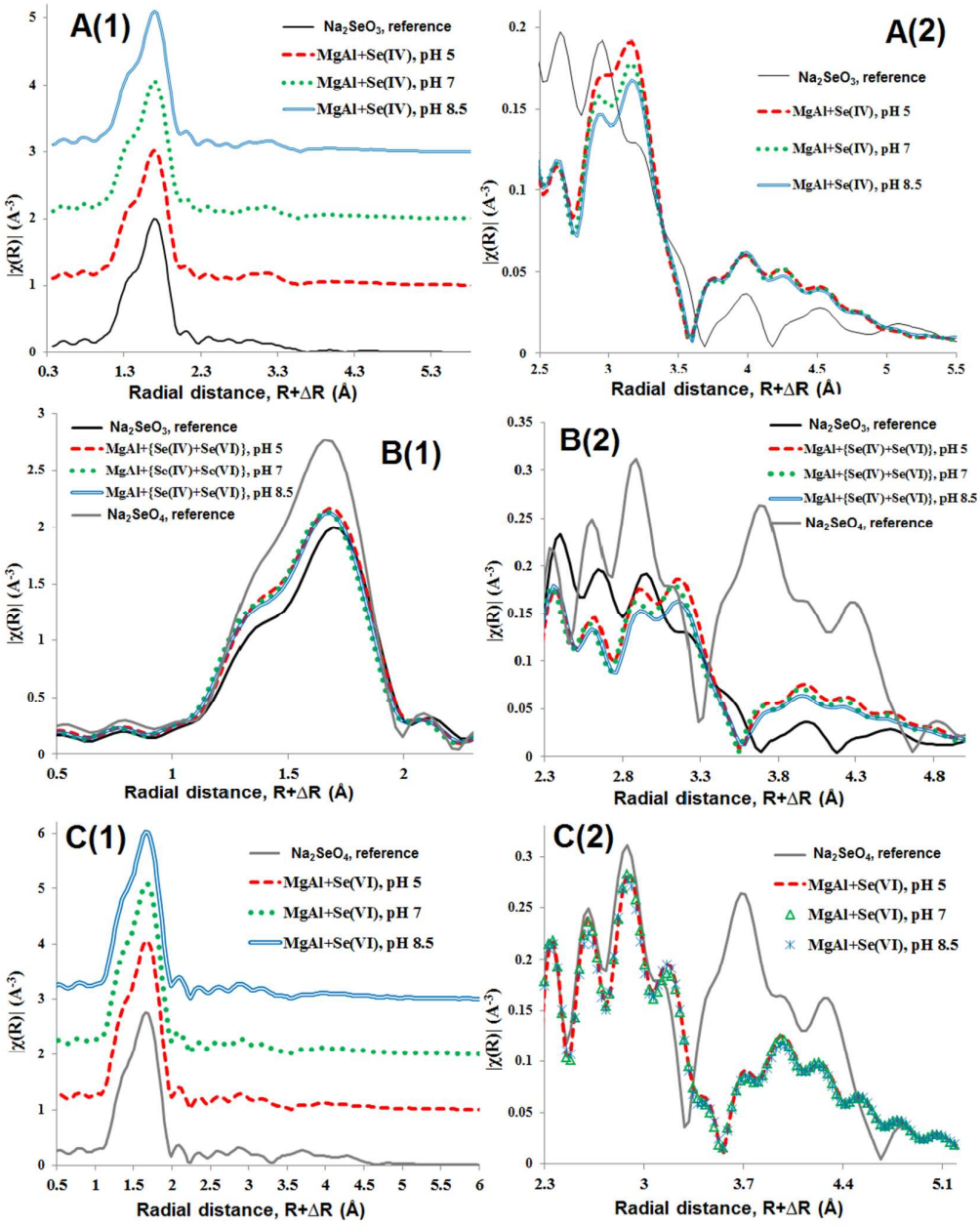

Fig. 5. The radial structure functions around selenium atom from the Fourier transforms of the EXAFS oscillation of the Se-sorbed Mg-Al LDHs in contact with (at pH 5, 7 and 8.5) $HSeO_3^-$ (A), both selenium aqueous species {Se(IV)+Se(VI)} (B) and SeO_4^{2-} (C) at 0.1-6.0 Å (1) and the second shell (2). *The Fourier transforms of {Se(IV)+Se(VI)}-sorbed HTs at 0.3-6.0 Å can be found in SI.*

The Se K-edge EXAFS are dominated by the oscillation from Se to O backscattering, which gives strong main peaks. The spectra of the Se(IV)-containing samples (Fig. 5A and 5B) show the second shell contributions, which are stronger at the lower pH values, as reflected by the higher peaks.

Calculations with Artemis and Feff. A number of theoretical samples with atomic coordinates calculated by our colleagues through X-ray crystallographic methods studies were used to generate Feff.inp files. Tables 1, 2 and 3 show the structural results for selenite, selenate and both selenium water species sorbed to Mg-Al LDHs resulting from EXAFS fitting by Artemis and Feff, respectively. All of the figures demonstrating the fittings (Figs. S2-S9) are included in the SI.

Selenite sorption. The main (strongest) peaks resulting from the oscillation from Se to O backscattering were easily fitted using three O atoms (CN=3.0-3.1) at 1.7 Å, indicating a trigonal pyramidal first-shell O configuration. The Se-O paths generated from the Feff.inp files using the relevant theoretical references, aluminum and magnesium selenite[18-19], gave the same results for the Se-O distance, coordination numbers and Debye-Waller factors (Table 1). That is, 1.7 Å is the theoretical Se-O distance in selenites calculated from the X-ray crystallography studies, EXAFS and quantum-chemistry computations.[18-23,40-42] The same Se-O distance of 1.7 Å was defined by EXAFS for the selenite sorbed to γ -Al_2O_3 calculated by Elzinga[40] and by aluminum hydrous oxide calculated by Peak.[41,42] These are the only EXAFS data on selenite and selenate sorption by adsorbents based on aluminum hydrous oxides.

The second shell (resulting from the oscillation of Se to Al and/or Mg backscattering) is shown by doublets at ~3 Å, reflecting Se-Al or/and Se-Mg distances (Fig. S2). Based on doublets in the second shell, one could consider two Se-Al/Mg distances resulting from the backscattering of Al/Mg located at different distances from the oscillating Se atom. To avoid incorrect assignments of the second shell backscattering, fittings of the first coordination shells to the Se-O paths were performed separately to determine whether oscillations from Se to O atoms are partly reflected in the second shell (Figs. S3 and S4). The smaller peak of the doublet at ~2.5 Å (uncorrected data),

which might have been considered a reflection of Al or Mg scattering, was fitted using the Se-O paths only. The fittings were performed with both k^3- and k^2-weighted χ data (Figures S3 and S4). The results suggest that only one reflection at ~2.8 Å (uncorrected distance) should be fitted using the Se-Al and Se-Mg paths. The smaller part of the doublet in the second shell area most likely results from O oscillations (Fig. S5).

Table 1. Structural parameters derived from Se K-edge EXAFS data of Se(IV)-sorbed Mg-Al LDHs by Artemis calculations using feff.inp files generated using the atomic coordinates of theoretical $Al_2(SeO_3)_3 \cdot 3H_2O$[18] and $MgSeO_3 \cdot 2H_2O$.[19] The amplitude reduction factor was $S_o^2=0.86$. R-interatomic distance, σ^2-the Debye-Waller mean square disorder factor, N-coordination number.

Sample	Se-O, first shell			Se-O, first shell		
MgAl+Se(IV)	Feff.inp from $Al_2(SeO_3)_3$			Feff.inp from $MgSeO_3$		
	R, Å	N	σ^2	R, Å	N	σ^2
pH=8.5	1.69(9)	3.1	.0018	1.69(8)	3.1	.0016
pH=7	1.69(6)	3.1	.0017	1.69(7)	3.1	.0019
pH=5	1.70(2)	3.0	.0018	1.69(8)	3.0	.0018
	Se-Al, second shell			Se-Mg, second shell		
	R, Å	N	σ^2	R, Å	N	σ^2
pH=8.5	3.21(3)	1.4	.0120	3.21(9)	1.4	.0040
pH=7	3.21(3)	1.5	.0110	3.21(0)	1.3	.0041
pH=5	3.21(8)	1.4	.0130	3.21(5)	1.2	.0042

The second shell indicated by the larger peak in the doublet was fitted using 1.4-1.5 Al atoms at 3.21 Å and pH 8.5 and 7 and at 3.22 Å at pH 5. It was also fitted using 1.2-1.4 Mg atoms at 3.22 Å at pH 8.5 and 5 and at 3.21 Å at pH 7. Similar results were calculated by our colleagues. The Se-Al distances for Se(IV)-Al_2O_3[40] and Se(IV) sorbed to hydrous aluminum oxide[41-42] were 3.20-3.22

Å and 3.21-3.22 Å, respectively, with no pH dependency. The coordination numbers for Se(IV) sorbed to γ-Al_2O_3 were found to range from 1.4 to 1.6[40] like in this work, which is most likely due to the domination of γ-Al_2O_3 among the aluminum species in the composition of Mg-Al LDH.

Selenate sorption. The Se K-edge EXAFS resulting from selenate sorption by Mg-Al LDH were fitted with 4.0-4.1 oxygen atoms at 1.65-1.645 Å (Table 2 and Fig. S6). At neutral and alkaline pH values, four O atoms were coordinated at 1.655 Å. At slightly acidic conditions, 4.1 oxygen atoms were coordinated at 1.645 Å.

Table 2. Structural parameters derived from Se K-edge EXAFS data of Se(VI)-sorbed Mg-Al LDHs calculated by Artemis using feff.inp files generated using the atomic coordinates of $[Al(H_2O)_6]_2(SeO_4)_3(H_2O)_4]$[20] and $MgSeO_4•6H_2O$.[23] The amplitude reduction factor was S_O^2=0.86. R - interatomic distance, σ^2 - the Debye-Waller mean square disorder factor, N - coordination number.

Sample	Se-O, first shell			Se-O, first shell		
MgAl+Se(VI)	Feff.inp from $Al_2(SeO_4)_3$			Feff.inp from $MgSeO_4$		
	R, Å	N	σ^2	R, Å	N	σ^2
pH=8.5	1.65(4)	4.05	0.0025	1.65(3)	4.05	0.0018
pH=7	1.65(7)	4.0	0.0016	1.65(6)	4.0	0.0015
pH=5	1.64(5)	4.1	0.0018	1.64(9)	4.1	0.0017

The Se K-edge EXAFS from selenite sorption were fitted using one (the first, 100% amplitude) path, Se-O (Fig. S6). There was no indication of Al/Mg backscattering at the second shell distance. These results were unexpected due to the unusually high adsorptive capacity of Mg-Al LDH toward selenate. To obtain more insight into the second shell possibilities for selenate sorbed to aluminum/magnesium hydrous oxides, several theoretical references calculated using Feff were carefully considered.[20-23] The purpose was to define at which distances we should expect the oscillations from the Se to Al/Mg backscattering. Feff.inp files were generated from hydrated

aluminum selenite[20-21], anhydrous aluminum selenate[22] and hydrated magnesium selenite.[23] Fig. S7 shows the paths of the Se-O and Se-Al/Mg generated from hydrated aluminum selenate (Fig. S7A), anhydrous aluminum selenate (Fig. S7B) and hydrated magnesium selenate (Fig. S7C). It was calculated that the nearest Se-Al and Se-Mg paths generated by Feff using the atomic coordinates of hydrated aluminum[20] and magnesium[23] selenates (as shown in Figs. S7A and S7C) have effective R values of 4.6-4.7 Å. The same Se-Al distance was calculated for another hydrated reference.[21] For such long distances between the atoms, inner sphere complexation cannot be take place.

In contrast, the Se-Al distances calculated using Feff for anhydrous aluminum selenate[22] were 3.25 - 3.38 Å (Fig. S7B). At such Se-Al distances, inner sphere complexation might formally take place, but for the same (anhydrous) theoretical reference, the Se-O distance (1.47 Å) is too short for a good fit of the first coordination shell of the experimental EXAFS (Fig. S7B).

Based on the Feff analysis of the oscillations from Se to Al backscattering using highly hydrated aluminum and magnesium selenates, we should not have expected an inner sphere complexation of selenate by the Mg-Al LDH, which is a highly hydrated adsorbent.

Sorption of both selenium aqueous species, selenite and selenate. Because both anions, selenite and selenate, were sorbed to Mg-Al LDHs, the Se K-edge EXAFS spectra show averaged data for both anions, which we cannot separate (Figs. 3B, 4B and 5B). The calculation of such EXAFS data was useful for understanding the sorption mechanism. The Artemis fitting of the EXAFS data for {Se(IV)+Se(VI)}-sorbed HTs was based on the (first calculated) fitting results for Se(IV)- and Se(VI)-sorbed samples (shown in Tables 1 and 2). Two paths (Se-O and Se-Al/Mg) from Se(IV) references[18-19] and one path (Se-O) from Se(VI) references[20,23] were used for the fitting, as shown in the SI (Figs. S8, S9). Table 3 summarizes the calculation results from Artemis. Fig. S8 shows the fits of {Se(IV)+Se(VI)}-sorbed Mg-Al LDHs using theoretical references for selenite and the paths resulting from Se oscillations to O and Al/Mg backscattering.[18-19]

Table 3. Structural parameters of {Se(IV)+Se(VI)} sorbed to MgAl-CO_3 LDHs from Se K-edge EXAFS data fitted by Artemis using feff.inp generated from $Al_2(SeO_3)_3 \cdot 3H_2O$[18], $MgSeO_3 \cdot H_2O$[19], $[Al(H_2O)_6]_2(SeO_4)_3(H_2O)_4]$[20] and $MgSeO_4 \cdot 6H_2O$.[23] The amplitude reduction factor was S_O^2=0.86. R - interatomic distance, σ^2 - the Debye-Waller mean square disorder factor, N - coordination number.

Sample	Se-O, first shell			Se-O, first shell		
MgAl+{Se(IV)&Se(VI)}	Feff.inp from $Al_2(SeO_3)_3$			Feff.inp from $MgSeO_3$		
	R, Å	N	σ^2	R, Å	N	σ^2
pH=8.5	1.69(0)	3.05	.0017	1.68(9)	3.05	.0015
pH=7	1.67(7)	3.15	.0017	1.68(1)	3.18	.0016
pH=5	1.67(3)	3.30	.0020	1.67(5)	3.33	.0019
	Se-Al, second shell			Se-Mg, second shell		
	R, Å	N	σ^2	R, Å	N	σ^2
pH=8.5	3.20(2)	0.8	.0035	3.20(0)	1.4	.0035
pH=7	3.19(5)	1.1	.0030	3.19(2)	1.2	.0088
pH=5	3.18(2)	1.4	.0020	3.18(7)	1.7	.0014
	Se-O, first shell			Se-O, first shell		
	Feff from $Al_2(SeO_4)_3$			Feff from $MgSeO_4$		
pH=8.5	1.68(9)	3.05	.0016	1.68(6)	3.06	.0018
pH=7	1.67(8)	3.15	.0017	1.67(9)	3.15	.0017
pH=5	1.67(7)	3.35	.0017	1.67(3)	3.30	.0022

Fig. S9 shows the fits using the theoretical references for selenates[20,23] when only the first coordination shells were fitted using the Se-O paths. Fitting the first coordination shell using the Se-O paths of all references gave the same results for the Se-O distances in the first shell: (average) 1.69, 1.68 and 1.67 at pH 8.5, 7 and 5, respectively (Table 3).

The data for the first coordination shells, which are shown in Tables 1, 2 and 3 for Se(IV), Se(VI) and the combination {Se(IV)+Se(VI)}, are plotted in Fig. 6, which allows a visual estimate of the contribution from each selenium aqueous species in the sorbed {Se(IV)+Se(VI)}-complex as a function of pH.

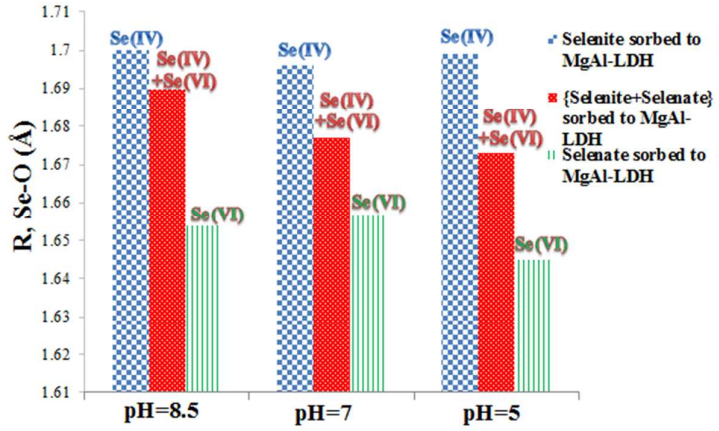

Fig. 6. Summary of the Se-O distances calculated from the Se K-edge EXAFS data of Mg-Al LDHs with sorbed selenite, selenate and {selenite+selenate} at pH 8.5, 7 and 5.

The data shown in Fig. 6 correlate with the Linear Combination fitting results for the sorption of two selenium oxyanions added simultaneously to experimental batches and reflects the ratio of Se(IV)-to-Se(VI) sorbed to Mg-Al LDHs as a function of pH. The portion of selenate in the sorbed complex increased as the pH decreased.

There was no Al/Mg backscattering in the Se K-edge EXAFS of the Se(VI)-sorbed samples (Figs. S6 and S7, Table 2), which means that the second shell reflections of {Se(IV)+Se(VI)}-sorbed Mg-Al LDHs resulted from only Se(IV) oscillations to Al/Mg atoms. However, when selenite was sorbed together with selenate, the Se-Al/Mg distances (of Se(IV)) became shorter than the Se-Al/Mg distances of solo sorbed Se(IV). Fig. 7 shows a decrease in the Se-Al/Mg distances of the Se(IV) companion sorption compared to only selenite sorption by the same inorganic ion exchanger at pH 8.5, 7 and 5.

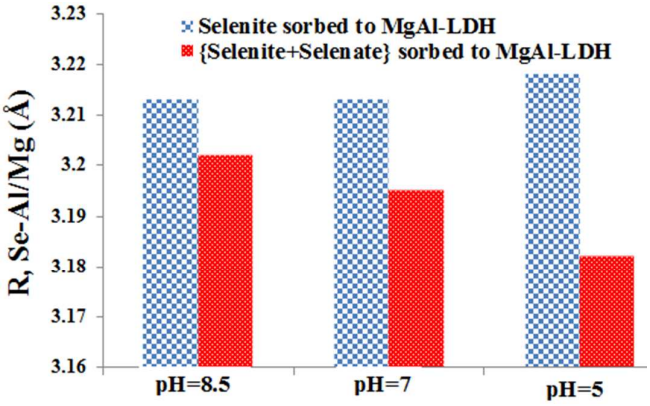

Fig. 7. The decrease in the Se(IV)-Al/Mg distances in the second coordination shell of Se based on the Se K-edge EXAFS of the Mg-Al LDHs resulting from the singly and combined sorption of selenite at pH 8.5, 7 and 5.

XRD patterns of the same samples are shown in Fig. S10 followed by the discussion on these data. XRD studies fully confirmed the results obtained by FTIR and EXAFS. It has been demonstrated that chemi-sorption is really the main mechanism of selenite removal by Mg-Al LDHs (Fig. S10C) but high removal capacity to selenate is due to involvement of the interlayer carbonate (Fig. S10A). Presence of selenite in the interlayer of HTs was less distinguished than of selenate. The presence of selenium aqueous species was reflected by the new peaks (at d=4.24-4.83 Å) indicating formation of multilayer within the interlayer space of the Mg-Al-CO_3 LDH. These new peaks are due to the presence of selenate in the interlayer space together with the interlayer carbonate of the Mg-Al-CO_3 LDHs, Fig. S10.

Discussion

The short answer to the first question (the role of the interlayer anions of Mg-Al-CO_3 LDH in selenium species removal) is 'yes': the interlayer carbonate was indeed always involved in the removal of selenite, selenate and both species added simultaneously to the experimental batches. However, the importance of the interlayer anions in the removal of one species was different than their importance for the removal of the other. The answer to the second question (goal) is that the

chemisorption mechanism did not dominate the removal of one of the investigated anions in spite of the high removal properties of Mg-Al LDH toward both aqueous selenium species.

Selenite. The very high adsorptive capacity of Mg-Al LDH toward selenite even at pH 8.5 (80 mg/g_{dw}), when selenite exists as SeO_3^{2-} (the most difficult species for adsorptive removal), is a result of a few processes occurring in a step-wise manner. Due to the high hydration and surface abundance of OH^- groups, the Se(IV) interactions at the Mg-Al LDH interface always begins with ion exchange of the surface OH^- for aqueous $HSeO_3^-$, which is reflected by an immediate pH increase. The further binding of selenite to HT was controlled by two processes: inner-sphere complexation and anion exchange of the interlayer CO_3^{2-}. The chemisorption mechanism for selenite removal by this material should be predicted from the shape of the adsorption isotherms (Fig. 1A), which are steep-like curves. The inner-sphere complexation was fully confirmed by the EXAFS analysis, which showed Se(IV)-Al/Mg distances of 3.21-3.22 Å fitted using a coordination number (CN) of 1.3-1.4 (Table 1, Figs. S2, S5). The values of the Se-Al/Mg distances and CNs at pH 5, 7 and 8.5 were close enough (slightly shorter at pH 8.5 and longer at pH 5), indicating no pH effect on the inner-sphere complexation. We hypothesize that inner-sphere complexation occurs via the oxygen from both Al and Mg. At the tested pH values, selenite was bound to Mg-Al LDH via a bidentate-binuclear (corner sharing) mechanism[40-43] and coordination to Al/Mg atoms via oxygen. These Se-Al distances are typical for hydrated aluminum oxides.[41]

The exceptionally high removal performance of Mg-Al LDH toward selenite was supported by the secondary anion exchange capacity of the layered hydroxides due to the interlayer carbonate ions. They gave a "second breath" to the HT adsorptive capacity at pH 5 by involving the less labile carbonate species shown at 1374 cm^{-1} (Fig. 2A). The modest involvement of the interlayer carbonate was the same at pH 8.5 and 7 (Fig. 2A) with different removal capacities (80 and 120 mg $[Se]/g_{dw}$, Fig. 1A), which indicates that inner-sphere complexation was the ruling mechanism for selenite removal. The released interlayer ions freed some additional adsorption sites, which resulted

in binding more Se(IV) ions. The number of additional adsorption sites was greater at pH 5, when the less easily exchangeable carbonate species were also released.

In summary, the reason for the higher selenite removal capacity by Mg-Al LDH is a combination of several properties of this material, such as an abundance of surface OH^-; semi-crystalline structure; lability of the interlayer carbonate species; and high hydration, which facilitates the participation of the interlayer carbonate in the removal. For selenite adsorption by Mg-Al LDH, the chemisorption mechanism was more important than the involvement of the interlayer carbonate.

Selenate. The FTIR and EXAFS analyses allowed the conclusion that the higher removal performance of Mg-Al LDH toward Se(VI) compared to the other adsorbents is fully provided by the interlayer ions what was confirmed by XRD studies (Fig. S10). The interlayer carbonate of Mg-Al LDH was exchanged with this tetrahedral anion in an amount proportional to the adsorptive capacity (Figs. 1B and 2C). Only one carbonate species with high lability, the monodentate form, was exchange at pH 8.5. Both carbonate species, shown at 1374 and 1515 cm^{-1}, were involved in the selenate removal. Nearly all of the interlayer carbonate was exchanged at pH 5, as indicated by the decrease in the bands at 1515 and 1374 cm^{-1}, which is also reflected by the appearance of new bands at 1010-1020 cm^{-1} that were assigned to the interlayer carbonate (Fig. 2C).

No inner sphere complexation of Se(VI) was detected during the EXAFS studies. Moreover, the analysis of the theoretical references (hydrated aluminum and magnesium selenate and anhydrous aluminum selenate) using Feff indicated that we should not even expect a chemisorption mechanism for selenate by the highly hydrated adsorbents based on aluminum and magnesium oxides. The nearest Se(VI)-Al and Se(VI)-Mg paths generated by Feff had too long Se-Al/Mg distances of 4.5-4.6 Å, which makes a chemisorption interaction impossible. This factor is most likely the reason for the low performance of many inorganic adsorbents toward selenate, which is usually much lower than that obtained toward selenite.

The EXAFS/Feff analysis of anhydrous aluminum selenate demonstrated that the inner-sphere complexation of selenate can, in principle, occur for adsorbents based on anhydrous aluminum oxides. However, the performance of these materials would be very low. Hydration is a very important quality for an inorganic ion exchanger to be able to sorb ions in technologically acceptable quantities. As a rule, the uptake is initiated by the ion exchange of H^+ (for cation exchangers) or OH^- (for anion exchangers). A lack of surface ion exchange groups results in negligible adsorption.

Peak experimentally demonstrated that hydrous aluminum oxides do not allow an inner-sphere complexation of selenate to occur, but he detected the inner-sphere complexation by corundum.[41] The adsorptive performance is not shown. Previous works by our colleagues[40-42] experimentally support this hypothesis.

In conclusion, the high removal capacity of Mg-Al LDH toward selenate is provided by the interlayer carbonate speciation and high hydration of the material. Selenate is removed by Mg-Al LDH solely via an ion exchange mechanism: the exchange of surface OH^- and the interlayer CO_3^{2-}.

Selenite versus selenate. It is clear now why the removal capacity of Mg-Al LDH for selenite was approximately twice that obtained for selenate (Figs. 1A and 1B). The uptake of selenate was a function of the ion exchange of surface OH^- and of the interlayer CO_3^{2-}. The sorption of selenite had a double support by the material compared to the sorption of selenate. Additionally, by taking advantage of the labile interlayer ions, selenite was supported by inner-sphere complexation, which always increases both the removal capacity and the affinity.

{Selenite+Selenate}. Both aqueous selenium species can be sorbed simultaneously by the Mg-Al LDH at pH 8.5, 7 and 5, as shown by the FTIR and EXAFS data. The ratio of Se(IV)-to-Se(VI) species attracted by this material depends on the mechanism of their removal, which is reflected in the adsorptive properties of Mg-Al LDH toward Se(IV) and Se(VI) (Figs. 1A and 1B).

A certain amount of each ion will always be attracted by any material of the same chemical nature as Mg-Al LDH that is characterized by an abundance of surface OH^- groups and a high porosity.

Further sorption of selenite by Mg-Al LDH is predominantly ruled by chemisorption with secondary support from the interlayer carbonate ions. Further sorption of selenate is fully dependent on the interlayer anions and their mobility/exchangeability at definite pH values. Because the two anions are sorbed by the Mg-Al LDH via different primary mechanisms, this material can pack both of them gently on the surface and in the interlayer with even less influence on the interlayer structure than obtained with the sorption of pure selenate. The portion of selenate in the {Se(IV)+Se(VI)}-sorbed complex increased from <10% (at pH 8.5) to 18% (pH 7) and 30.5% (pH 5) (Fig. 6) in accordance with the increase in the lability of the interlayer anions. We cannot ignore the higher affinity of Mg-Al LDH toward selenite than toward selenate, which is reflected in its inner sphere complexation to this material. This property will always result in better sorption in any competitive adsorption compared to another ion that lacks the chemisorption mechanism, which is the reason that the ratio of Se(IV)-to-Se(VI) in the sorbed {Se(IV)+Se(VI)} complex does not strictly correlate with the adsorptive capacities shown in Figs. 1A and 1B.

The presence of selenate in the interlayer reduced the Se(IV)-Al/Mg distances (Fig. 7), but the changes were not strong enough to change the geometry of the inner sphere complexes of selenite. Se-Al/Mg distances of 3.18-3.22 Å indicate bidentate binuclear complexation to the surface.[41]

Multilayer formed within the interlayer of Mg-Al-CO_3 LDHs due to sorption of selenium aqueous species did not violate the structure of this HT (Fig. S10). The interlayer distance (7.74 Å) and the other XRD patterns reflecting its layered structure were not changed after sorption of selenate and selenite. It is an indication that the adsorbent is strong enough what makes it suitable for water treatment.

Conclusions

Mg-Al-CO_3 Layered Double Hydroxide prepared via an alkoxide-free sol-gel method demonstrated high adsorptive performance toward aqueous selenite and selenate at the pH values of natural and purifying drinking water. This material removes selenite at capacities of 80, 120 and 160 mg [Se]/g_{dw} and selenate at capacities of 30, 45 and 90 mg [Se]/g_{dw} at pH 8.5, 7 and 5, respectively.

This technologically attractive performance is due to a combination of several properties of Mg-Al LDH provided by the synthetic method. These properties are a high surface reactivity, which is underpinned by generous speciation; high porosity; labile carbonate species in the interlayer and high hydration, which allows the interlayer carbonate to be exchanged with selenium aqueous species.

The high removal performance of Mg-Al LDH toward both selenium species would not be possible without the involvement of the interlayer carbonate. The interlayer CO_3^{2-} played an important role in the removal of selenite, but it was a major mechanism for selenate adsorption by the Mg-Al LDH.

Chemisorption was the leading mechanism for selenite removal, but inner-sphere complexation was not detected for selenate adsorption to Mg-Al LDH.

Mg-Al LDH is easily able to sorb both selenite and selenate simultaneously. This is particularly easy due to the different sorption mechanisms for these two species.

Due to its high removal capacity, Mg-Al LDH developed using the alkoxide-free sol-gel approach can be used to recover selenium from wastewaters that contain either aqueous selenium species or both of them together. This material can also be used in water treatment to reduce these species to concentration less than 10 μg/L due to its high affinity toward selenite and selenate.

Acknowledgments

A major part of the work was funded by King Abdullah University of Science and Technology (KAUST) through Center-in-Development award N^{o} KUK-C1-017-12. The EXAFS research at DUBBLE at ESRF was funded by NWO (Dutch Ministry of Scientific Research). The authors gratefully thank Dr. Harrison (University of Aberdeen) and Prof. Krivovichev (St. Petersburg State University) for providing the crystallography data.

Notes and References

[1*]School of Engineering and Built Environment, Glasgow Caledonian University, Cowcaddens Road 70, G40BA, Glasgow, Scotland, United Kingdom
E-mail: Natalia.Chubar@gcu.ac.uk
[2]Department of Earth Sciences, Faculty of Geosciences, Utrecht University, Budapestlaan 4, 3584CD, Utrecht, The Netherlands

ESI (Electronic Supplementary Information) containing ten figures and description is available online.

References

1. Q. Wang, D. O'Hare, *Chem. Reviews,* 2012, **112**, 4124.
2. Z. Li, B. Yang, S. Zhang, B. Wang, B. Xue, *J. Mater. Chem. A***,** 2014, **2,** 10202**.**
3. Y. Li, L. Zhang, Z. Hiang, D. Yan, F. Li, *J. Mater. Chem. A***,** 2014, DOI: 10.1039/C4TA01275E
4. Q. Fang, B. Chen, *J. Mater. Chem. A*, 2014, **2**, 8941.
5. V. Oestreicher, M. Jobbágy, *Langmuir***,** 2013**, 29** (39*),* 12104.
6. S. Ma, Q. Chen, H. Li, P. Wang, S.M. Islam, Q. Gu, X. Yang, M.G. Kanatzidis, *J. Mater. Chem. A*, 2014, **2**, 10280.

7. D. Hoyo, *Appl. Clay Scie*., 2007, **36**, 103.
8. T. Posati, V. Benfenati, A. Sagnella, A. Pistone, M. Nocchetti, A. Donnadio, G. Ruani, R. Zamboni, M. Muccini, *Biomacromolecules*, 2014, **15**, 158.
9. R. Ma, J. Liang, K. Takada, T. Sasaki, *J. Am. Chem. Soc*., 2011, **133**, 613.
10. S.J. Palmer, R.L. Frost, T.M. Nguyen, *Coord. Chem. Rev.*, 2009, **253**, 250.
11. N. Chubar, V. Gerda, O. Megantari, M. Mičušík, M. Omastova, K. Heister, P. Man, J. Fraissard, J. *Chem. Eng. J.,* 2013, **234,** 284.
12. X. Yuan, Y. Wang, J. Wang, C. Zhou, Q. Tang, X. Rao, *Chem. Eng. J., 2013*, **221**, 204.
13. Y. Kuroda, Y. Miyamoto, M. Hibino, K. Yamaguchi, N. Mizuno, *Chem. Mater*., 2013**, 25**, 2291.
14. N. Chubar, *J. Coll. Interf. Sci.,* 2011*,* **357**, 198.
15. Review of available technologies for the removal of selenium from water. North American Metals Council, June **2010**, prepared by Sandy, T.; DiSante, C. (http://www.namc.org/docs/00062756.PDF. Last visited August 7, 2014)
16. S. Nikitenko, A. Beale, A. van der Eerden, S. Jacques, U. Leynaud, M. Óbrien, D. Detollenaere, R. Kaptein, B. Weckhuysen, W. Bras, *J. Synchrotron Radiation,* 2008, **15**, 632.

17. B. Ravel, M. Newville, *J. Synchrotron Radiation,* 2005, **12**, 537.
18. W.T.A. Harrison, G.D. Stucky, R.E. Morris, A.K. Cheetam, *Acta Cryst.* 1992, **48**, 1365.
19. M.G. Johnston, W.T.A. Harrison, *Acta Cryst*., 2001, **E57**, i24-i25.
20. S.B. Krivovichev, *Proceedings of the Russian Minerol. Soc*., 2006**, 2**, 106. (in Russian)
21. G. Jonansson, *Acta Chemica Scandinavica,* 1962, **16**, 403.
22. R. Perret, B. Rosso, *Bull. Soc. Chim. Fr.* 1968, 2700.
23. U. Kolitsch, *Acta Cryst. Section B*, 2002, **58**, i3.
24. N. Takeno, Geological Survey of Japan Open File Report No. 419, May **2005**.
25. G. Jegadeesan, K. Mondal, S.B. Lalvani, *Environ. Technol*. 2003, **24**, 1049.
26. Y.T. Chan, W.H. Kuan, T.Y. Chen, M.K. Wang, *Water Res*., 2009, **43**, 4412.
27. S.S. Dash, K.M. Parida, *J. Coll. Interf. Scie*., 2007, **307**, 333.
28. M. Szlachta, N. Chubar, *Chem. Eng. J.,* 2013, **217**, 159.
29. S. Mandal, S. Mayadevi, B.D. Kulkarni, *Ind. Eng. Chem. Res.,* 2009, 48*,* 7893.
30. J.S. Yamani, A.W. Lounsbury, J.B. Zimmerman, *Water Res*., 2014, **50**, 373.
31. N. Bleiman, Y.G. Mishael, *J. Haz. Mat*., 2010, **183**, 590.
32. S.M. Das, M.J. Hendry, Essilfie-Dughan, *J. Appl. Geochem*., 2013, **28**, 185.
33. L. Gaini, M. Lakraimi, E. Sebbar, A. Meghea, M. Bakasse, *J. Haz. Mat.,* 2009, **161**, 627.
34. I.F. Myronyuk, V.O. Kotsyubynsky, V.L. Chelyadyn, J.Y. Kostin, U.Y. Dgura, *Physics and Chemistry of Solid State,* 2009, **10**, 848 (in Ukrainian)
35. W.B. White, *The Amer. Mineralogist,* 1971, **56**, 46.
36. H. Wijnja, C.I. Schulthess, *J. Coll. Interf. Scie*., 2000, **229**, 286.
37. C. Su, D. Saurez, *Soil Sci. Soc. Am. J*., 2000, **64**, 101.
38. G. Lefevre, Adv. *Coll. Interface Scie*., 2004, **107**, 109.
39. A.A. Hosseini, A. Niaei, S. Salari, *Open J. Phys. Chem*., 2011, **1**, 23.
40. E.J. Elzinga, Y. Tang, J. McDonald, S. DeSisto, R.J. Reeder, *J. Coll. Interf. Scie.,* 2009, **340**, 153.
41. D. Peak, *J. Coll. Interf. Sci*., 2006, **303**, 337.
42. D. Peak, U.K. Saha, P.M. Huang, *Soil Sci. Soc. Am. J.,* 2006, ***70***, 192.
43. J.A. Ippolito, K.G. Scheckel, K.A. Barbarick, *J. Coll. Interf. Sci.,* 2009, **338**, 49.

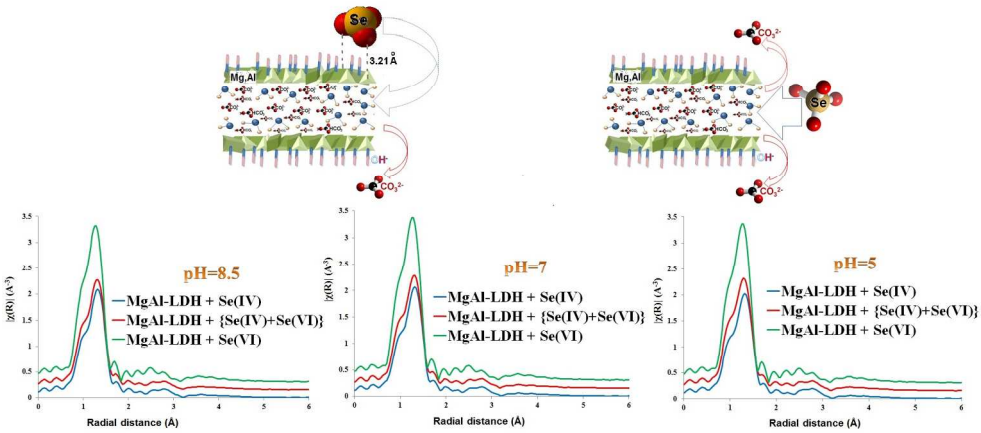

This work is the first theoretical explanation of why it is more difficult to sorb selenate than selenite.
368x165mm (144 x 144 DPI)